NEW ORBITAL ELEMENTS FOR ACCURATE PROPAGATION IN THE SOLAR SYSTEM

Baù Giulio, Andrea Milani

University of Pisa
Department of Mathematics
Largo Pontecorvo 5, 56127 Pisa

Davide Amato, Claudio Bombardelli

Technical University of Madrid
Department of Applied Physics
Plaza Cardenal Cisneros 3, 28040 Madrid

ABSTRACT

In this paper we present new variables to describe the orbital motion of a celestial body in the Solar System. The motion is the solution of a perturbed two-body problem, where the main perturber can be the Sun or any planet. Two sets of generalized orbital elements are proposed for positive and negative values of the total energy, respectively. The former is the subject of the paper [1], while the latter is here presented for the first time. Numerical tests for perturbed geocentric motion and close encounters with a planet show that the new coordinates are very efficient when compared with both regularized and Cowell's methods.

Index Terms— orbital propagation, close encounters, regularization

1. INTRODUCTION

Close encounters with massive bodies, such as planets or Jupiter/Saturn's satellites, make the orbit of any asteroid or spacecraft chaotic. Moreover, in the case of subsequent encounters the Lyapunov time can become very short. Accurate propagation is required in the orbit determination of chaotic bodies, because it mitigates the exponential divergence of nearby orbits. For example, the impact monitoring of natural and artificial objects with the Earth, and the planning of space missions with several fly-bys, have to be done with mathematical tools that are able to deal with chaos. One of these tools is a reliable and accurate orbit propagator.

We propose new methods to accurately compute elliptic and hyperbolic motion in the Solar System. Our approach roots in the regularization of the two-body equation, which is transformed into a set of linear differential equations with constant coefficients. This result is obtained by introducing a new independent variable (also called fictitious time) and new spatial coordinates in place of the position and velocity.

In the Burdet-Ferrándiz linearization the fictitious time is the true anomaly, and the new state variables are the inverse of the orbital radius, the radial direction and the angular momentum. In this way the motion is decomposed into the radial displacement and the rotation of the radial unit vector. We show that a new linearization of the two-body equation can be obtained with a similar decomposition when either the eccentric or the hyperbolic anomaly is the independent variable. Then, by applying the variation of parameters we introduce six variables that can be used to describe the perturbed motion of the propagated object. The new quantities, together with the total energy and the physical time, constitute the state vector of the special perturbation methods proposed here. We also investigate the geometrical and physical meaning of the six parameters: they are all related to an intermediate frame which shares with the local-vertical local-horizontal frame the direction of the angular momentum. This slowly moving frame recalls the ideal frame discovered by the Danish astronomer P. A. Hansen in 1857, which plays a key role in Deprit's ([2]) and Peláez's ([3]) sets of orbital elements.

The method that works with negative values of the total energy is presented in Section 2. The new variables are introduced by following a geometrical approach. The connection with a new linearization of the two-body problem is explained in [1]. A similar formulation for positive values of the total energy is presented, for the first time, in Section 3. The performance of the new formulations has been evaluated for geocentric motion and for interplanetary orbits with close encounters. Some results are reported in Section 4.

2. GENERALIZED ELLIPTIC MOTION

We adopt throughout this paper non-dimensional quantities such that the product of the gravitational constant and the total mass of the two bodies is equal to one. Let us describe the dynamical state of the propagated body by its position $\mathbf{r}$ and velocity $\mathbf{v}$ relative to the central body (also called "primary"). They are expressed in a coordinate system with the origin at the primary's centre of mass and with fixed axes in space. In general, the moving particle is acted upon by the force $\mathbf{F}$

$$\mathbf{F} = -\frac{\mathbf{r}}{r^3} - \frac{\partial \mathcal{U}\left(t,\, \mathbf{r}\right)}{\partial \mathbf{r}} + \mathbf{P}\left(t,\, \mathbf{r},\, \mathbf{v}\right), \tag{1}$$

where the disturbing potential energy $\mathcal{U}$ is assumed to be independent on the velocity and $\mathbf{P}$ includes any perturbation that does not arise from a disturbing potential.

Let the vector $\mathbf{h}$ be the orbital angular momentum and the scalars r and h be the magnitudes of $\mathbf{r}$ and $\mathbf{h}$, respectively. We define the *orbital* frame $\mathcal{O} = \{\mathrm{F};\, \mathbf{i},\, \mathbf{j},\, \mathbf{k}\}$ by means of the orthonormal basis

$$\mathbf{k} = \frac{\mathbf{h}}{h}, \qquad \mathbf{i} = \frac{\mathbf{r}}{r}, \qquad \mathbf{j} = \mathbf{k} \times \mathbf{i}, \tag{2}$$

which rotates at the angular velocity

$$\mathbf{w}_{\mathcal{O}} = N\,\frac{r}{h}\,\mathbf{i} + \frac{h}{r^2}\,\mathbf{k}. \tag{3}$$

Then, it is straightforward to write the velocity vector as

$$\mathbf{v} = \frac{\mathrm{d}r}{\mathrm{d}t}\,\mathbf{i} + \frac{h}{r}\,\mathbf{j}. \tag{4}$$

It is convenient to express also the perturbing force vector $\mathbf{F}$ in the orbital frame:

$$\mathbf{F} = \left(R - \frac{1}{r^2}\right)\mathbf{i} + T\,\mathbf{j} + N\,\mathbf{k}. \tag{5}$$

Finally, the total energy is given by

$$\varepsilon = \frac{1}{2}\mathbf{v}^2 - \frac{1}{r} + \mathcal{U}. \tag{6}$$

In Section 2 we assume that $\varepsilon < 0$.

2.1. The intermediate frame

We define the generalized eccentricity vector as

$$\mathbf{g} = -\mathbf{i} + \mathbf{w} \times \mathbf{c}, \tag{7}$$

where $\mathbf{w}$ and $\mathbf{c}$ denote the generalized velocity and angular momentum vectors, respectively:

$$\mathbf{w} = \frac{\mathrm{d}r}{\mathrm{d}t}\,\mathbf{i} + \frac{c}{r}\,\mathbf{j}, \quad \mathbf{c} = c\,\mathbf{k}, \quad c = \sqrt{h^2 + 2\,r^2\,\mathcal{U}}. \tag{8}$$

The magnitude of $\mathbf{g}$, which is computed from (7), (8) by taking into account of (6), reads

$$g = \sqrt{1 + 2\,\varepsilon\,c^2}, \tag{9}$$

with $0 \le g < 1$. The orientation of $\mathbf{g}$ on the orbital plane can be represented by the generalized true anomaly θ:

$$g\cos\theta = \frac{c^2}{r} - 1, \qquad g\sin\theta = c\,\frac{\mathrm{d}r}{\mathrm{d}t}. \tag{10}$$

The angle θ is reckoned from $\mathbf{g}$ up to the radial direction $\mathbf{i}$ counterclockwise with respect to $\mathbf{k}$ (see Figure 1). In analogy with the definition of the osculating eccentric anomaly, we introduce the generalized eccentric anomaly G as follows:

$$g\cos G = 1 + 2\,\varepsilon\,r, \qquad g\sin G = r\,\sqrt{-2\,\varepsilon}\,\frac{\mathrm{d}r}{\mathrm{d}t}. \tag{11}$$

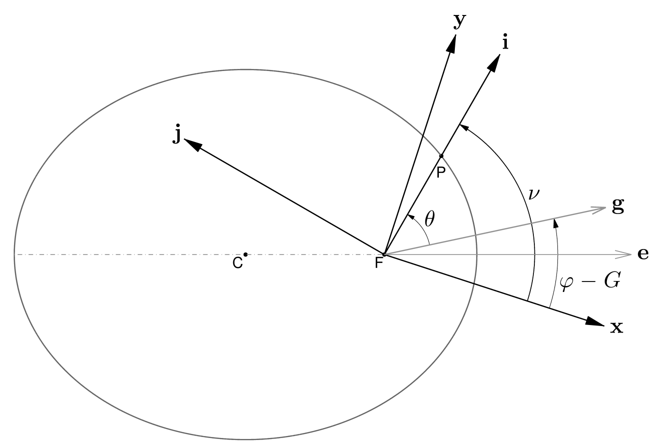

Fig. 1. The intermediate frame $\{\mathrm{F};\, \mathbf{x},\, \mathbf{y},\, \mathbf{k}\}$ as viewed from the $\mathbf{k}$ axis (see 2). The propagated object P occupies one point of the instantaneous osculating ellipse with centre in C and one focus in F. The generalized eccentricity vector $\mathbf{g}$ (eq. 7) coincides with the osculating eccentricity vector $\mathbf{e}$ only if $\mathcal{U} = 0$. In the case $\mathcal{U} \neq 0$ they share the same direction only if $\frac{\mathrm{d}r}{\mathrm{d}t} = 0$. This picture is taken from [1].

Let us consider the unit vectors

$$\mathbf{x} = \mathbf{i}\,\cos\nu - \mathbf{j}\,\sin\nu, \tag{12}$$
$$\mathbf{y} = \mathbf{j}\,\cos\nu + \mathbf{i}\,\sin\nu, \tag{13}$$

where the vectors $\mathbf{i}$, $\mathbf{j}$ belong to the orbital frame $\mathcal{O}$ and

$$\nu = \varphi + \theta - G. \tag{14}$$

Next, we introduce the *intermediate* frame $\mathcal{I} = \{\mathrm{F};\, \mathbf{x},\, \mathbf{y},\, \mathbf{k}\}$ where $\mathbf{k} = \mathbf{x} \times \mathbf{y}$ is perpendicular to the orbital plane (see 2). The direction of $\mathbf{x}$ locates the departure point from which the longitude ν of the propagated object is measured (see Figure 1). The relative angular velocity of $\mathcal{I}$ with respect to $\mathcal{O}$ is

$$\boldsymbol{\omega}_{\mathcal{I}\mathcal{O}} = -\frac{\mathrm{d}\nu}{\mathrm{d}t}\,\mathbf{k}, \tag{15}$$

and its absolute angular velocity results

$$\boldsymbol{\omega}_{\mathcal{I}} = \boldsymbol{\omega}_{\mathcal{O}} + \boldsymbol{\omega}_{\mathcal{I}\mathcal{O}} = N\,\frac{r}{h}\,\mathbf{i} + \left(\frac{h}{r^2} - \frac{\mathrm{d}\nu}{\mathrm{d}t}\right)\mathbf{k}, \tag{16}$$

where $\boldsymbol{\omega}_{\mathcal{O}}$ and N are given in (3) and (5).

The intermediate frame $\mathcal{I}$ is not an ideal frame, since the component of the angular velocity $\boldsymbol{\omega}_{\mathcal{I}}$ along $\mathbf{k}$ is not identically zero. Besides, the attitude of $\mathcal{I}$ is influenced, in general, not only by N, as for the ideal frames developed in [2] and [3], but also by the in-plane projections of $\mathbf{F}$ (i.e. R and T, see 5).

2.2. New orbital elements

The independent variable is represented by φ which is related to the physical time t by

$$\frac{\mathrm{d}t}{\mathrm{d}\varphi} = \frac{r}{\sqrt{-2\,\varepsilon}}. \tag{17}$$

The first two orbital elements λ_1 and λ_2 of the proposed method are the projections of $\mathbf{g}$ along the vectors $\mathbf{x}$ and $\mathbf{y}$ of the intermediate frame

$$\lambda_1 = g\,\cos(\varphi - G)\,, \tag{18}$$
$$\lambda_2 = g\,\sin(\varphi - G)\,, \tag{19}$$

so that

$$\mathbf{g} = \lambda_1\,\mathbf{x} + \lambda_2\,\mathbf{y}. \tag{20}$$

An other element is the generalized semi-major axis

$$\lambda_3 = -\frac{1}{2\,\varepsilon}. \tag{21}$$

The four Euler parameters λ_4, λ_5, λ_6, λ_7 are chosen to track the evolution of the orthonormal basis $(\mathbf{x},\,\mathbf{y},\,\mathbf{k})$. This frame shares with the orbital frame the direction $\mathbf{k}$ of the angular momentum vector. Therefore, its relative orientation to the orbital frame is a rotation around $\mathbf{k}$ of the angle ν between $\mathbf{x}$ and the radial unit vector $\mathbf{i}$. Such angle is determined from the elements λ_1, λ_2, λ_3 and the independent variable. These quantities also characterize the motion along $\mathbf{i}$. The last missing information is about the magnitude of the angular momentum. In general, this is a function of the whole set of elements through the disturbing potential energy. Finally, the set of seven spatial elements is completed by a time element λ_0 in order to compute the physical time in a more efficient way.

We collect below the differential equations of the eight variables of the new method:

$$\frac{\mathrm{d}\lambda_{0,l}}{\mathrm{d}\varphi} = \lambda_3^{3/2}\left[1 + (R\,r - 2\,\mathcal{U})\,r + 2\,\Lambda_3\,\zeta\right], \tag{22}$$

$$\frac{\mathrm{d}\lambda_1}{\mathrm{d}\varphi} = (R\,r - 2\,\mathcal{U})\,r\,\sin\varphi + \Lambda_3\left[(1+\varrho)\cos\varphi - \lambda_1\right], \tag{23}$$

$$\frac{\mathrm{d}\lambda_2}{\mathrm{d}\varphi} = (2\,\mathcal{U} - R\,r)\,r\,\cos\varphi + \Lambda_3\left[(1+\varrho)\sin\varphi - \lambda_2\right], \tag{24}$$

$$\frac{\mathrm{d}\lambda_3}{\mathrm{d}\varphi} = 2\,\lambda_3^3\left(R_p\,\zeta + T_p\,n + \frac{\partial\mathcal{U}}{\partial\,t}\,\sqrt{\lambda_3}\varrho\right), \tag{25}$$

$$\frac{\mathrm{d}}{\mathrm{d}\varphi}\begin{pmatrix}\lambda_4\\ \lambda_5\\ \lambda_6\\ \lambda_7\end{pmatrix} = N\,\frac{r^2}{2\,n}\begin{pmatrix}\lambda_7\,c_\nu - \lambda_6\,s_\nu\\ \lambda_6\,c_\nu + \lambda_7\,s_\nu\\ -\lambda_5\,c_\nu + \lambda_4\,s_\nu\\ -\lambda_4\,c_\nu - \lambda_5\,s_\nu\end{pmatrix} + \frac{\omega_z}{2}\begin{pmatrix}\lambda_5\\ -\lambda_4\\ \lambda_7\\ -\lambda_6\end{pmatrix}, \tag{26}$$

where

$$r = \lambda_3\,\varrho, \tag{27}$$

$$c_\nu = \cos\nu,\quad s_\nu = \sin\nu,\quad \nu = \varphi + 2\arctan\left(\frac{\zeta}{m+\varrho}\right), \tag{28}$$

$$\omega_z = \frac{n-m}{\varrho} + \frac{1}{m\,(1+m)}\left[(2\,\mathcal{U} - R\,r)\,(2 - \varrho + m)\,r + \Lambda_3\,\zeta\,(\varrho - m)\right], \tag{29}$$

and

$$\Lambda_3 = \frac{1}{2\lambda_3}\,\frac{\mathrm{d}\lambda_3}{\mathrm{d}\varphi}, \tag{30}$$

$$\varrho = 1 - \lambda_1\cos\varphi - \lambda_2\sin\varphi,\quad \zeta = \lambda_1\sin\varphi - \lambda_2\cos\varphi, \tag{31}$$

$$n = \sqrt{m^2 - 2\,\lambda_3\varrho^2\,\mathcal{U}},\qquad m = \sqrt{1 - \lambda_1^2 - \lambda_2^2}. \tag{32}$$

Since ν appears only as the argument of trigonometric functions, it is possible to avoid (28) and directly employ the expressions

$$\varrho\,c_\nu = \cos\varphi - \lambda_1 + \frac{\zeta\,\lambda_2}{m+1},\quad \varrho\,s_\nu = \sin\varphi - \lambda_2 - \frac{\zeta\,\lambda_1}{m+1}. \tag{33}$$

Moreover, given the perturbing force $\mathbf{F}$ (eq. 1) we have

$$R = \mathbf{F}\cdot\mathbf{i},\quad N = \mathbf{F}\cdot\mathbf{k},\quad R_p = \mathbf{P}\cdot\mathbf{i},\quad T_p = \mathbf{P}\cdot\mathbf{j}, \tag{34}$$

where $\mathbf{i}$, $\mathbf{j}$, $\mathbf{k}$ are obtained from the new orbital elements as shown in sect. 5.2 of [1]. Note that we report only the differential equation of the linear time element $\lambda_{0,l}$, the one for the constant time element can be found in [1].

The system (22)–(26) holds for negative values of the total energy (ε). Additionally, we require that the potential $\mathcal{U}\,(t,\,\mathbf{r})$ satisfies $c^2 > 0$, where c is the generalized angular momentum (see 8; this issue is discussed in [4], sect. 6). The conditions $\varepsilon < 0$, $c \neq 0$ imply that $g < 1$ (eq. 9), and, since $m^2 = 1 - g^2$ (from 18, 19, 32), we have in particular $m \neq 0$, thus avoiding the singularity in (29). Finally, equations (26) become singular when $h = 0$.

Remark. In both methods presented in this work and in [4] the disturbing potential energy $\mathcal{U}$ is assumed to be independent on the velocity $\mathbf{v}$. However, this hypothesis could be relaxed since what we really ask is that $\mathcal{U}$ is independent on the osculating angular momentum h, which enters the component of $\mathbf{v}$ along the transverse vector $\mathbf{j}$.

3. GENERALIZED HYPERBOLIC MOTION

We describe the formulation for positive values of the total energy ($\varepsilon > 0$). The derivation follows a different approach with respect to the previous section. Here we emphasize the connection of the orbital elements with a new linearization of the two-body problem.

In the Burdet-Ferrándiz linearization the motion is seen as the composition of the radial displacement r along the unit vector **i** (r and **i** are also called "projective coordinates") with the rotation of **i** in space. The inverse of r and the components of **i** obey second-order linear differential equations with constant coefficients when the independent variable is switched from the physical time to the true anomaly.

The general idea from which we start to obtain the methods presented in this paper is to combine the projective decomposition with a time transformation of Sundman type.

3.1. Radial motion

The Newtonian equation of motion of the propagated body is readily obtained by computing the acceleration from (4) and considering the force as given in (5). Then, projection along **i** yields

$$\frac{\mathrm{d}^2 r}{\mathrm{d}t^2} = \frac{h^2}{r^3} - \frac{1}{r^2} + R. \tag{35}$$

We want to transform (35) into a linear differential equation and then apply the variation of constants technique. To this end let us first introduce a new independent variable through the time transformation

$$\frac{\mathrm{d}t}{\mathrm{d}\varphi} = \frac{r}{\sqrt{2\,\varepsilon}}. \tag{36}$$

The total energy ε is expressed by means of (4) and (8) as

$$2\,\varepsilon = \left(\frac{\mathrm{d}r}{\mathrm{d}t}\right)^2 + \left(\frac{c}{r}\right)^2 - \frac{2}{r}, \tag{37}$$

where $c^2 = h^2 + 2\,r^2\,\mathcal{U}$. In the case of Keplerian motion the quantity φ represents the hyperbolic anomaly up to an additive constant. The radial velocity and acceleration become

$$\frac{\mathrm{d}r}{\mathrm{d}t} = \frac{\sqrt{2\,\varepsilon}}{r}\,\frac{\mathrm{d}r}{\mathrm{d}\varphi}, \tag{38}$$

$$\frac{\mathrm{d}^2 r}{\mathrm{d}t^2} = \frac{2\,\varepsilon}{r^2}\left[\frac{\mathrm{d}^2 r}{\mathrm{d}\varphi^2} - \frac{1}{r}\left(\frac{\mathrm{d}r}{\mathrm{d}\varphi}\right)^2\right] + \frac{1}{r^2}\,\frac{\mathrm{d}r}{\mathrm{d}\varphi}\,\frac{\mathrm{d}\varepsilon}{\mathrm{d}\varphi}. \tag{39}$$

Next, equation (38) is employed into (37) and after rearranging the terms we find the useful relation

$$\left(\frac{\mathrm{d}r}{\mathrm{d}\varphi}\right)^2 = r^2 + \frac{r}{\varepsilon} - \frac{c^2}{2\,\varepsilon}. \tag{40}$$

Using (39) and (40) we can write (35) in the following form:

$$\frac{\mathrm{d}^2 r}{\mathrm{d}\varphi^2} - r - \lambda_3 = (R\,r - 2\,\mathcal{U})\,\lambda_3\,r + \frac{1}{2\lambda_3}\,\frac{\mathrm{d}\lambda_3}{\mathrm{d}\varphi}\,\frac{\mathrm{d}r}{\mathrm{d}\varphi}, \tag{41}$$

where we have introduced the generalized semi-major axis λ_3

$$\lambda_3 = \frac{1}{2\,\varepsilon}. \tag{42}$$

From the well-known relation for the time derivative of the total energy ([5], p. 11, eq. 16, wherein h is replaced by $-\varepsilon$) we get

$$\frac{\mathrm{d}\lambda_3}{\mathrm{d}\varphi} = -2\,\lambda_3^{5/2} r\left(\mathbf{P}\cdot\mathbf{v} + \frac{\partial\,\mathcal{U}}{\partial\,t}\right), \tag{43}$$

with $\partial/\partial t$ denoting the partial derivative with respect to time. Note that the right-hand side of equation (43) vanishes when perturbations are not applied ($\mathcal{U}$ and $\mathbf{P}$ are both equal to zero).

We conclude that by introducing the fictitious time φ through the differential transformation (36) and exploiting the total energy integral in the form provided by relation (40) we regularized equation (35) at least in the unperturbed part. This result lays the ground for introducing the first set of orbital elements of the method proposed for positive energy.

3.2. Orbital elements λ_1, λ_2, λ_3

In absence of perturbations equation (41) reduces to the linear differential equation of an harmonic oscillator of unitary frequency perturbed by the constant term λ_3:

$$\frac{\mathrm{d}^2 r}{\mathrm{d}\varphi^2} = r + \lambda_3. \tag{44}$$

Therefore, we seek a solution of (44) in the form

$$r = \lambda_3\left(\lambda_1 \cosh\varphi + \lambda_2 \sinh\varphi - 1\right), \tag{45}$$

$$\frac{\mathrm{d}r}{\mathrm{d}\varphi} = \lambda_3\left(\lambda_1 \sinh\varphi + \lambda_2 \cosh\varphi\right), \tag{46}$$

where λ_1 and λ_2 are integration constants. From the latter relation, by using the former one, we obtain the following condition

$$\frac{\mathrm{d}\lambda_1}{\mathrm{d}\varphi}\cosh\varphi + \frac{\mathrm{d}\lambda_2}{\mathrm{d}\varphi}\sinh\varphi = -\frac{\varrho}{\lambda_3}\,\frac{\mathrm{d}\lambda_3}{\mathrm{d}\varphi}, \tag{47}$$

where, for convenience, we introduce the auxiliary quantity

$$\varrho = \lambda_1 \cosh\varphi + \lambda_2 \sinh\varphi - 1. \tag{48}$$

Moreover, according to the method of variation of constants we can substitute the solution given by (45) and (46) into equation (41) regarding the coefficients as unknown functions of φ. We obtain

$$\frac{\mathrm{d}\lambda_1}{\mathrm{d}\varphi}\sinh\varphi + \frac{\mathrm{d}\lambda_2}{\mathrm{d}\varphi}\cosh\varphi = (R\,\lambda_3\varrho - 2\,\mathcal{U})\,\lambda_3\varrho - \Lambda_3\left(\lambda_1 \sinh\varphi + \lambda_2 \cosh\varphi\right), \tag{49}$$

where Λ_3 was defined in (30). The system of equations (47), (49) can be solved with respect to the derivatives of λ_1 and λ_2 to have

$$\frac{\mathrm{d}\lambda_1}{\mathrm{d}\varphi} = -\left(R\,r - 2\,\mathcal{U}\right) r\,\sinh\varphi + \Lambda_3\left[(1-\varrho)\cosh\varphi - \lambda_1\right], \tag{50}$$

$$\frac{\mathrm{d}\lambda_2}{\mathrm{d}\varphi} = \left(R\,r - 2\,\mathcal{U}\right) r\,\cosh\varphi + \Lambda_3\left[(\varrho-1)\sinh\varphi - \lambda_2\right], \tag{51}$$

where we have replaced $\lambda_3\varrho$ with r.

The quantities λ_1, λ_2, λ_3 are chosen as state variables of the new formulation. By use of (4), (38), (46) we convert equation (43) in

$$\frac{\mathrm{d}\lambda_3}{\mathrm{d}\varphi} = -2\,\lambda_3^{5/2}\left[R_p\,\zeta\,\sqrt{\lambda_3} + T_p\,h + \frac{\partial\,\mathcal{U}}{\partial\,t}\,r\right], \tag{52}$$

where $R_p = \mathbf{P}\cdot\mathbf{i}$, $T_p = \mathbf{P}\cdot\mathbf{j}$, and

$$\zeta = \lambda_1\sinh\varphi + \lambda_2\cosh\varphi. \tag{53}$$

The generalized angular momentum can be obtained from the compact formula (from 40 with the aid of 45, 46)

$$c^2 = \lambda_3\left(\lambda_1^2 - \lambda_2^2 - 1\right), \tag{54}$$

so that for the osculating angular momentum h we have

$$h^2 = \lambda_3\left(\lambda_1^2 - \lambda_2^2 - 1 - 2\,\mathcal{U}\,\lambda_3\varrho^2\right). \tag{55}$$

Note that h depends also on $\mathbf{i}$ through the disturbing potential energy $\mathcal{U}\,(t,\,r\,\mathbf{i})$.

In order to completely determine the dynamics of the propagated body we need to compute the vectors $\mathbf{i}$ and $\mathbf{j}$ of the orbital frame.

3.3. The intermediate frame

The definitions of the generalized eccentricity vector $\mathbf{g}$ and of the true anomaly θ provided in (7) and (10), respectively, still hold for $\varepsilon > 0$. In particular, we note that $g > 1$ (see 9). Moreover, we recall that θ is the angle reckoned from $\mathbf{g}$ to the radial direction $\mathbf{i}$, counterclockwise with respect to $\mathbf{k}$.

Let the generalized hyperbolic anomaly F be defined by

$$g\cosh F = 1 + 2\,\varepsilon\,r, \qquad g\sinh F = 2\,\varepsilon\,\frac{\mathrm{d}r}{\mathrm{d}\varphi}. \tag{56}$$

Then, from (45), (46), and using (56) these expressions for λ_1 and λ_2 can be found:

$$\lambda_1 = g\,\cosh\left(F-\varphi\right), \tag{57}$$

$$\lambda_2 = g\,\sinh\left(F-\varphi\right). \tag{58}$$

We introduce the angle

$$\alpha = \frac{1}{2}\,\mathrm{gd}\left(2\,F - 2\,\varphi\right), \tag{59}$$

where the function $\mathrm{gd}\,(x)$ denotes the Gudermannian of x ([6], p. 165). We have

$$(\cos\alpha,\,\sin\alpha) = \frac{1}{\gamma}\left(\lambda_1,\,\lambda_2\right), \quad \tan\alpha = \tanh\left(F-\varphi\right), \tag{60}$$

where

$$\gamma = \sqrt{\lambda_1^2 + \lambda_2^2}. \tag{61}$$

Then, the vector $\mathbf{g}$ can be written as

$$\mathbf{g} = \frac{g}{\gamma}\left(\lambda_1\,\mathbf{x} + \lambda_2\,\mathbf{y}\right), \tag{62}$$

where $\mathbf{x}$ and $\mathbf{y}$ are two orthonormal vectors. Assume that $\mathbf{x}\times\mathbf{y} = \mathbf{k}$, with $\mathbf{k}$ defined in (2). As in the case $\varepsilon < 0$ we consider the intermediate frame $\mathcal{I} = \{\mathrm{F};\,\mathbf{x},\,\mathbf{y},\,\mathbf{k}\}$. The orientation of this frame with respect to the orbital frame is set by the angle

$$\nu = \theta + \alpha \tag{63}$$

through the projections

$$\mathbf{i}\cdot\mathbf{x} = \cos\nu, \qquad \mathbf{i}\cdot\mathbf{y} = \sin\nu. \tag{64}$$

Therefore, the angular velocity of $\mathcal{I}$ relative to the orbital frame has the same expression shown in (15) where ν is now taken from (63).

3.4. Orbital elements λ_4, λ_5, λ_6, λ_7

We represent the orientation of the intermediate frame $\mathcal{I}$ with respect to a fixed reference frame by the Euler parameters λ_4, λ_5, λ_6, λ_7. They obey first-order differential equations that have the same form reported in (26), where $n^2 = m^2 - 2\,\lambda_3\varrho^2\,\mathcal{U}$ and

$$m = \sqrt{g^2 - 1}, \qquad g = \sqrt{\lambda_1^2 - \lambda_2^2}. \tag{65}$$

Moreover, we have

$$s_\nu = \sin\nu = \frac{1}{\varrho\,\gamma\,g}\left[\lambda_2(m^2-\varrho) + \lambda_1\,m\,\zeta\right], \tag{66}$$

$$c_\nu = \cos\nu = \frac{1}{\varrho\,\gamma\,g}\left[\lambda_1(m^2-\varrho) - \lambda_2\,m\,\zeta\right], \tag{67}$$

and the quantity

$$\omega_z = \frac{\mathrm{d}t}{\mathrm{d}\varphi}\left(\boldsymbol{\omega}_{\mathcal{I}}\cdot\mathbf{k}\right), \tag{68}$$

is computed by the formula

$$\omega_z = \frac{n-m}{\varrho} - \frac{r}{m}\left(R\,r - 2\,\mathcal{U}\right)\left[1 + (\varrho+1)\left(\frac{1}{g^2} + \frac{m}{\gamma^2}\right)\right] - \zeta\,\Lambda_3\left[\frac{\varrho-1}{\gamma^2} + \frac{1}{g^2}\left(m + \frac{\varrho}{m}\right)\right]. \tag{69}$$

It could be proved that the elements λ_4, λ_5, λ_6, λ_7 are "attached" to an other set of four Euler parameters, which obey linear first-order differential equations.

We conclude that the evolution of the radial and transverse vectors (**i**, **j**) can be determined from the seven orbital elements λ_i, $i = 1...7$. This information together with the motion along **i** allow to track the position and velocity of the propagated body with respect to a known reference frame.

3.5. Time element

The physical time can be obtained by (numerical) integration of equation (36). An other possibility, which is described in this section, is to employ a time element. We write (36) as

$$\frac{\mathrm{d}t}{\mathrm{d}\varphi} = \lambda_3^{3/2}\varrho. \tag{70}$$

In the case of pure Keplerian motion λ_1, λ_2, and λ_3 are constants, and integration of (70) by separation of variables yields

$$t = \lambda_{0,c} + \lambda_3^{3/2}\left(\lambda_1 \sinh\varphi + \lambda_2\cosh\varphi - \varphi\right). \tag{71}$$

The constant $\lambda_{0,c}$ can be regarded as a time element. If the motion is perturbed $\lambda_{0,c}$ changes with φ, and its derivative is

$$\frac{\mathrm{d}\lambda_{0,c}}{\mathrm{d}\varphi} = \lambda_3^{3/2}\left[\Lambda_3\left(3\,\varphi - 2\,\zeta\right) - \left(R\,r - 2\,\mathcal{U}\right)r\right]. \tag{72}$$

An alternative time element $\lambda_{0,l}$ can be defined by

$$\lambda_{0,l} = \lambda_{0,c} - \varphi\,\lambda_3^{3/2}. \tag{73}$$

Either the "constant" ($\lambda_{0,c}$) or the "linear" ($\lambda_{0,l}$) time element can be included among the state variables instead of the physical time itself.

4. RESULTS

We report the results for two benchmark problems. The first one is a geocentric motion along an highly eccentric orbit under gravitational perturbations. The second one is an heliocentric orbit characterized by a deep close encounter with the Earth. The formulation for negative values of the total energy has been extensively tested in [1], and, in fact, the results in Section 4.1 are taken from that paper.

4.1. Geocentric motion

The osculating eccentricity and inclination at the initial epoch are about 0.95 and 30 degrees, and the spacecraft occupies the perigee of the orbit at a distance of 6800 km from the Earth's centre of mass. Two perturbations are active: the Earth's oblateness and the Moon's gravitational attraction. This example has been used by several authors and, as far as we know, it first appears in [5] (p. 118).

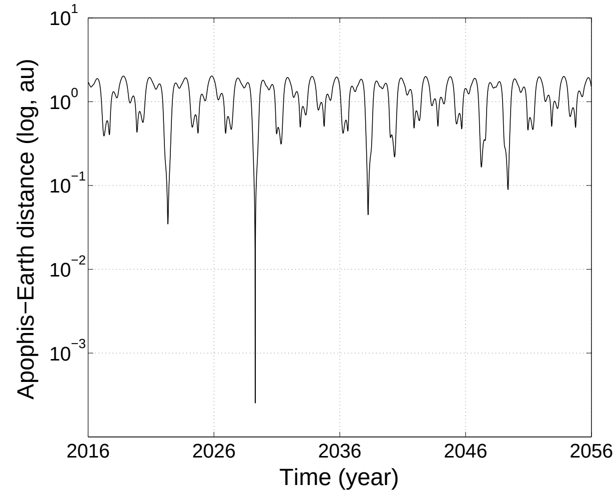

Fig. 4. Evolution of the distance between Apophis and the Earth throughout 40 years starting from January 1, 2016.

We investigate the relation between the accuracy in the position at a given epoch and the computational cost. The selected numerical integrator is the Runge–Kutta (4, 5) pair of Dormand and Prince, hereafter called DOPRI54. An important feature of it is that the length of the stepsize is controlled by relative and absolute tolerances. The computational cost is measured by the total number of evaluations of the right-hand side of the differential equations (functions calls). Let us pick a time of propagation corresponding to a final position close to the farthest point from the Earth of the fiftieth revolution. Figure 2 displays the variation in the position error as the relative tolerance of DOPRI54 is modified inside a suitable range thus producing a consequent variation of the number of function calls. The proposed method is the most efficient since it requires the smallest computational effort for a given accuracy.

The performance in a long-term propagation, here of five thousand periods of the initial Keplerian ellipse, is shown in Figure 3. In this test we chose multistep methods with fixed stepsize (more informations are given in [1], sect. 7.2). It is notable that at the end of the propagation New is more accurate than the Kustaanheimo-Stiefel (KS) regularization and the set of elements of Stiefel and Scheifele (Sti&Sche) of one and two orders of magnitude, respectively.

A much more detailed description of the two numerical tests can be found in [1]. In particular, we refer to sect. 7.1 and table 1 for the formulations compared to the new one.

4.2. Heliocentric orbit with planetary close encounters

We analyze the effect on the orbital propagation accuracy of the close encounter between the asteroid (99942) Apophis and the Earth on April 13, 2029. The estimated minimum

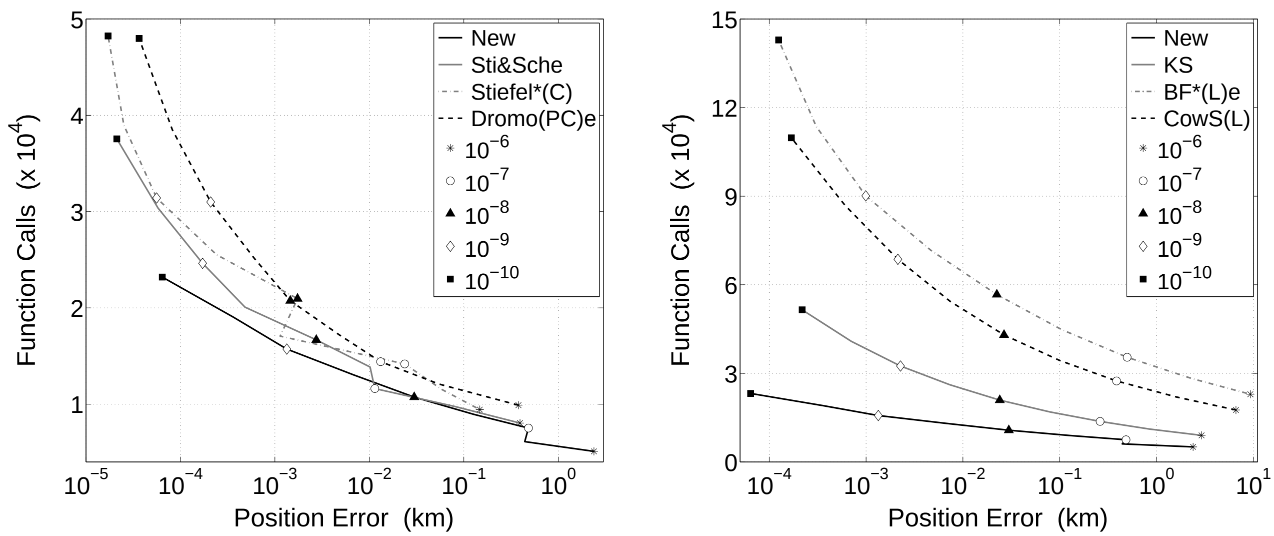

Fig. 2. Function calls versus position error after 288.12768941 msd (about 49.5 revolutions). The relative tolerance of DOPRI54 is changed from 10^{-6} to 10^{-10}, and the absolute tolerance is set to 10^{-13}. The new method is compared with formulations based on elements (left) and on coordinates (right). These pictures are taken from [1].

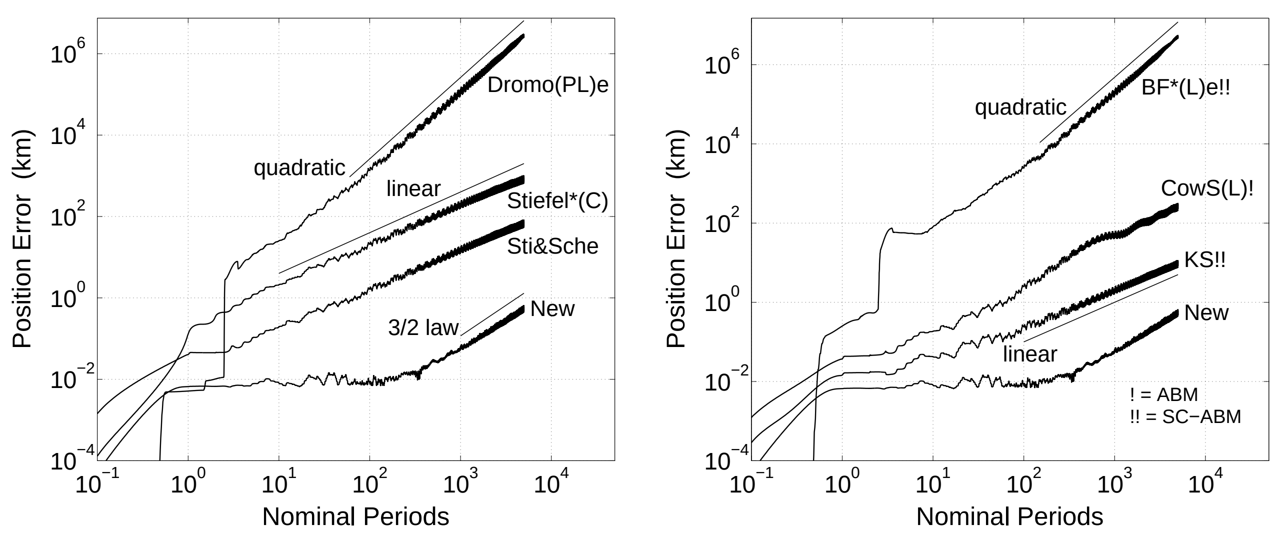

Fig. 3. Position error accumulated during 5000 periods of the initial osculating ellipse. The new method is compared with formulations based on elements (left) and on coordinates (right). The numerical integrators are the 10th-order multistep methods ABM, SC-ABM, and the number of steps per period is 144. These pictures are taken from [1].

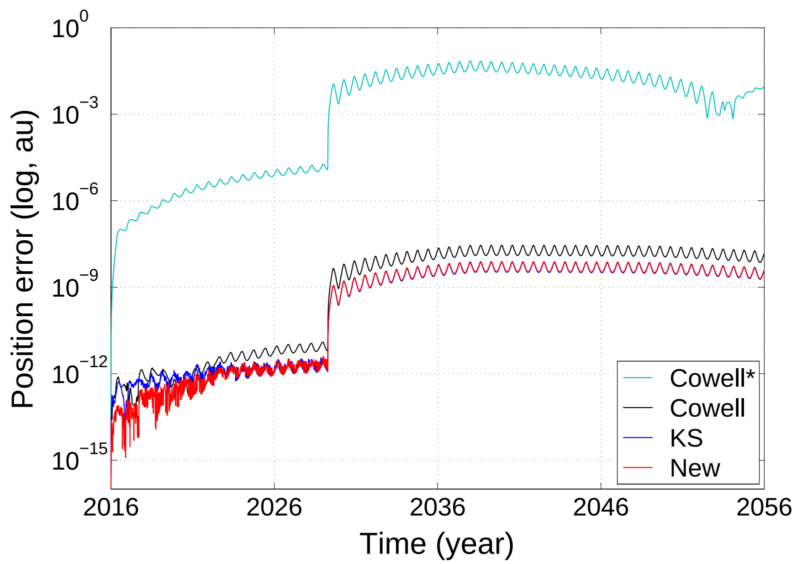

Fig. 5. Heliocentric position error accumulated in 40 years of propagation. The new formulations are compared with Cowell's method and the Kustaanheimo-Stiefel regularization. A multistep algorithm with variable stepsize and order is used, and two values of the relative tolerance are considered: 10^{-9} (Cowell*), and 10^{-15} (Cowell, KS, New).

distance, available in the NEODyS website, is almost 0.0003 astronomical units (au). We decided a time interval of integration of 40 years, starting from January 1, 2016. In our simple dynamical model the asteroid is acted upon by the gravitational attractions of the Sun and the Earth, which is on a circular orbit.

The following strategy is applied with the two new formulations. When the Earth-Apophis distance is bigger than 0.018 au, the Earth is the perturbing body. Otherwise, the primary body is switched from the Sun to the Earth, so that the former becomes the perturber. We expect that the formulation working for $\varepsilon < 0$ (Section 2) is used in the heliocentric phase, and the other one (Section 3) in the geocentric arc of trajectory. Cowell's method and the Kustaanheimo-Stiefel regularization [5] are also considered in our analysis. For these methods we do not change the primary which remains always the Sun. The numerical integrator is a multistep implicit Adams-Moulton scheme with variable stepsize and order [7].

An accurate integration was carried out with Cowell's method in quadruple precision and with tight values of the absolute and relative tolerances. We checked that only in the close encounter of 2029 the minimum distance goes below 0.018 au (see Figure 4). This propagation provided us a "reference" orbit for computing the error. Moreover, it also allowed us to determine the initial position and velocity of the asteroid and the Earth in order to reproduce the close encounter on April 13, 2029.

In Figure 5 we show the error in the heliocentric position throughout the whole time span of propagation. Two different settings of the numerical integrator are taken for Cowell's method. Table 1 reports the total number of function calls for each propagation. It is notable that with a comparable computational cost the new propagator is 6 orders of magnitude more accurate than Cowell's method at the end of the integration. Moreover, even by increasing the number of function calls of a factor 4, Cowell is still less accurate than New. The methods proposed in this work can reach the same accuracy as KS with slightly less function calls.

Table 1. Function calls of the propagations shown in Figure 5

Method	10^{-9}	10^{-15}
New	–	12544
KS	–	13658
Cowell	15083	45249

4.3. Total energy transitions

The performance of the formulations presented in Sections 2 and 3 can deteriorate for values of the energy ε close to zero. This situation happens for example if ε changes its sign. A possible solution is to include in the propagator a third formulation that works for any value of the energy. A good candidate is represented by the method Dromo ([3], [4]). In practice, when $|\varepsilon|$ is smaller than a given threshold the propagation is carried out by Dromo.

5. CONCLUSIONS

New formulations of the perturbed two-body problem are proposed. One method, which was published in [1], holds for a negative total energy of the propagated body. An other formulation, presented here for the first time, works for positive values of the total energy. The position and velocity are replaced by seven spatial elements and a time element. The new quantities root in a new linearization of the two-body problem. This is achieved by combining the projective decomposition approach adopted in the Burdet-Ferrándiz regularization with a time transformation of order one instead of two (here "order" refers to the exponent of the orbital radius). We show that the seven spatial variables can be defined by means of an intermediate frame, which shares with the local-vertical local-horizontal frame the direction of the angular momentum vector. Two numerical tests, for geocentric motion and for a heliocentric orbit with close encounters, show the very good performance of the new formulations when compared to Cowell's method and other regularized schemes both based on elements and on coordinates.

6. REFERENCES

[1] G. Baù, C. Bombardelli, J. Peláez, and E. Lorenzini, "Non-singular orbital elements for special perturbations in the two-body problem," *Monthly Notices of the Royal Astronomical Society*, vol. 454, pp. 2890–2908, 2015.

[2] A. Deprit, A. Elipe, and S. Ferrer, "Ideal Elements for Perturbed Keplerian Motions," *Journal of research of the National Bureau of Standards, 79B*, pp. 1–15, 1975.

[3] J. Peláez, J.M. Hedo, and P.R. de Andrés, "A special perturbation method in orbital dynamics," *Celestial Mechanics and Dynamical Astronomy*, vol. 97, pp. 131–150, 2007.

[4] G. Baù, C. Bombardelli, and J. Peláez, "A new set of integrals of motion to propagate the perturbed two-body problem," *Celestial Mechanics and Dynamical Astronomy*, vol. 116, pp. 53–78, 2013.

[5] E.L. Stiefel and G. Scheifele, *Linear and Regular Celestial Mechanics*, Springer-Verlag, New York Heidelberg Berlin, 1971.

[6] R.H. Battin, *An Introduction to the Mathematics and Methods of Astrodynamics*, AIAA Education Series, AIAA, Reston, VA, revised edition, 1999.

[7] K. Radhakrishnan and A.C. Hindmarsh, "Description and Use of LSODE, the Livermore Solver for Ordinary Differential Equations," Tech. Rep. UCRL-ID-113855, Lawrence Livermore National Laboratory, Washington, D. C., 1993.